Acta Physiologiae Plantarum (2018) 40:23
https://doi.org/10.1007/s11738-017-2598-z

ORIGINAL ARTICLE

The cellular pathway and enzymatic activity for phloem-unloading transition in developing *Camellia oleifera* Abel. Fruit

Xiaoyi Wang[1] · Hanli You[1] · Yihang Yuan[1] · Hehua Zhang[1] · Lingyun Zhang[1]

Received: 5 January 2017 / Revised: 13 December 2017 / Accepted: 20 December 2017 / Published online: 4 January 2018

Abstract

The phloem-unloading pathway of sucrose and mechanism of sugar-to-oil transition are still unknown in *Camellia oleifera* Fruit. Here, transmission electronic microscopy (TEM) and confocal laser-scanning microscopy (CLSM) were used to observe the cellular structure of vascular bundles and symplastic tracer, carboxyfluorescein (CF), transport in phloem zone. The results showed that sucrose was transported via symplast system in the early and late phases, whereas apoplast system exerted the function in middle stage. Moreover, enzymatic assays showed that acid invertase had a higher activity at the transition stage during the whole fruit development. The cell wall bound invertase (CWI) activity reached the highest at the middle stage of fruit development and the switch in phloem-unloading coincided with fruit developmental phase change and oil accumulation. Correlation analysis showed that the oil accumulation was significantly negatively correlated with content of soluble sugar at $P < 0.05$ level. However, the soluble acid invertase (SAI), CWI, and neutral invertase showed a significant positive correlation with oil accumulation at $P < 0.01$ level. In summary, our data provide new cytological insights into the transition of unloading transfer between symplasmic and apoplasmic patterns in *C. oleifera* fruit and suggest that invertases are positively involved in sugar–oil transition process.

Keywords Phloem unloading · Sugar accumulation · Oil accumulation · Invertase · *Camellia oleifera*

Introduction

Sugar partitioning in plant is regulated by some complicated and various physiological processes such as photosynthesis, phloem transport and unloading, etc. The partitioning of photoassimilates and maintenance of sink strength which are closely related to phloem unloading to a great degree determine the yield and quality of crop (Oparka 1990; Patrick 1997). The mechanisms and route of sugar phloem transport have been heretofore extensively discussed in a relative number of species and a variety of sink organs including vegetative sink and reproductive sink organs. Oil crops such as oil tea (*Camellia oleifera*) are a type of crops that are used to extract oil as the main purpose. However, comparing with fresh fruits and vegetative tissues, the mechanism of phloem transport in oil crops remains unknown. Oil tea is one of the most economically important plant with a high level of edible and healthy camellia oil, known as 'oriental olive oil' (Zeng et al. 2013). The content of unsaturated fatty acids in seed of oil tea is over 80% which is higher than that of olive oil (Wang et al. 2012). Oleic acid has the highest level in oil tea, followed by linoleic acid. The saturated fatty

Communicated by U. Feller.

Xiaoyi Wang and Hanli You equal contributors.

Electronic supplementary material The online version of this article (https://doi.org/10.1007/s11738-017-2598-z) contains supplementary material, which is available to authorized users.

✉ Lingyun Zhang
lyzhang@bjfu.edu.cn

Xiaoyi Wang
231736841@qq.com

Hanli You
youhanli@bjfu.edu.cn

Yihang Yuan
yuanyihang@126.com

Hehua Zhang
zhanghehua1991@126.com

[1] Key Laboratory of Forest Silviculture and Conservation of the Ministry of Education, Beijing Forestry University, Beijing 100083, People's Republic of China

acid includes palmitic acid and stearic acid. So far, the oil accumulation mechanism in *C. oleifera* fruit remains poorly understood.

In general, phloem-unloading pathway includes symplasmic, apoplasmic, or simultaneous symplasmic and apoplasmic unloading route. Photoassimilate transport through the complex boundary of SE–CC first, and then transfer through a variety of parenchyma cells into the sink. Symplasmic or an alternative apoplasmic unloading route is involved in the process of SE unloading. Nevertheless, photoassimilate transport not only via symplasmic but also apoplasmic pathways synchronously, which have already been explored in several species such as apple, Chinese jujube, and blueberry (Nie et al. 2010; Zhang et al. 2004, 2016). The symplasmic route has been proved to be predominant in most tissues (Oparka and Cruz 2000; Viola et al. 2001), especially in vegetative storage sinks (Imlau et al. 1999) and developing seeds (Aoki et al. 2006; Haupt et al. 2001). The symplasmic route depends on plasmodesmata connecting different cells and is associated with lower resistance and greater transport capacity (Patrick 1997). Both tissue type and the development stage can largely determine the conductivity of plasmodesmata that connect SE–CC cells to parenchyma cells (Turgeon and Wolf 2009). The apoplasmic route is dependent on carrier-mediated sugar transporters and closely related to enrichment of soluble sugars in sink (Turgeon and Wolf 2009). Apoplasmic phloem transport is almost impossible to happen in strong sinks for the movement of the *trans*-membrane solute which require transporters and energy (Haupt et al. 2001). Apoplasmic route predominates in many sink organs which represent the other kind of sinks that contain a strong storage capacity. It was demonstrated that apoplasmic phloem-unloading pathway was employed through fruit development in such fruits as *Malus pumila* (Zhang et al. 2004), *Actinidia chinensis* (Chen et al. 2017), and *Vaccinium corymbosum* (Zhang et al. 2016). However, more changeable unloading pattern and relatively complicated unloading mechanism were found in a variety of reproductive storage sink organs. Phloem transport changed from symplasmic to apoplasmic routes just when the fruit turn to ripen by CF transport and GFP-tagged viral movement protein in *Vitis vinifera* (Zhang et al. 2006), whereas two shifts between apo-symplasmic unloading transfer were present in jujube fruit with fruit development (Nie et al. 2010). In peach, sucrose was transported via an apoplasmic pathway both in the early and middle stages during the development of fruit (Zanon et al. 2015).

Since sugar transporter-mediated movement largely participate in apoplasmic transfer and retrieve from sieve element cell to apoplast space, a variety of sugar transporters have been identified in many species. In litchi, LcSUT4 is involved in apoplasmic transport to promote sugar accumulation in litchi aril (Wang et al. 2015). Sucrose transporters SWEETs are involved in apoplasmic transport. AtSWEET11, 12, and 15 mediated the sucrose transport from seed coat to embryo (Chen et al. 2015). The transition of unloading route is definitely associated with the developmental stage of sink and physiological conditions; however, the potential mechanisms in the transition based on the cellular and biochemical level remain unknown especially in *C. oleifera* fruit. Cevdet et al. analyzed the relationship among sugar, organic acids, and oil content during olive development. They reported that the total sugar was positively related to organic acid ($P < 0.01$), but the positive correlation was at a low level between the contents of oil and total organic acids ($P < 0.05$) in olive varieties (Nergiz and Ergonul 2009). However, little is known about sugar–oil transition mechanism in *C. oleifera* fruit.

In the study, we investigated the phloem-unloading pathway and mechanism in *C. oleifera* during fruit development. We demonstrated the dual switch between sym- and apoplasmic unloading route. Furthermore, the data provide evidence that invertases are positively involved in sugar–oil transition process.

Materials and methods

Plant materials

Camellia oleifera Abel. Fruits (variety 'xianglin 11') were collected from the Forestry Research Institute of Hunan Province in China for the experiments. The variety 'xianglin 11' blossomed in late November in each year. Since the ovary went into dormancy after fruit setting, the fruit developmental curve was plotted from April 1st in the next year when the fruits resumed growth. Most samples were collected on the basis of the growth curve of *C. oleifera* fruit 'xianglin 11' in the year of 2012–2013 at different developmental stages: early developmental stage (20 weeks after anthesis), rapid growing stage (30 weeks after anthesis), oil accumulation, and fruit full-blown stage (35 weeks after anthesis) (Fig. 1). The fruits were harvested at different stages for analysis of acid invertase, soluble sugar, and the content of oil and processed immediately with liquid nitrogen and then stored at – 80 °C.

Tissue preparation and observation for ultrastructure

The tissue for structural observation was prepared according to (Zhang et al. 2006). Briefly, the vascular bundles of *C. oleifera* fruit were cut into 2–3 mm^3 pieces with a double-sided blade and then fixed with 5% (v/v) glutaraldehyde immediately in a 100 mM pre-cooled phosphate buffer (pH 7.0) for 6 h. After three 3-min rinses in the pre-cooled

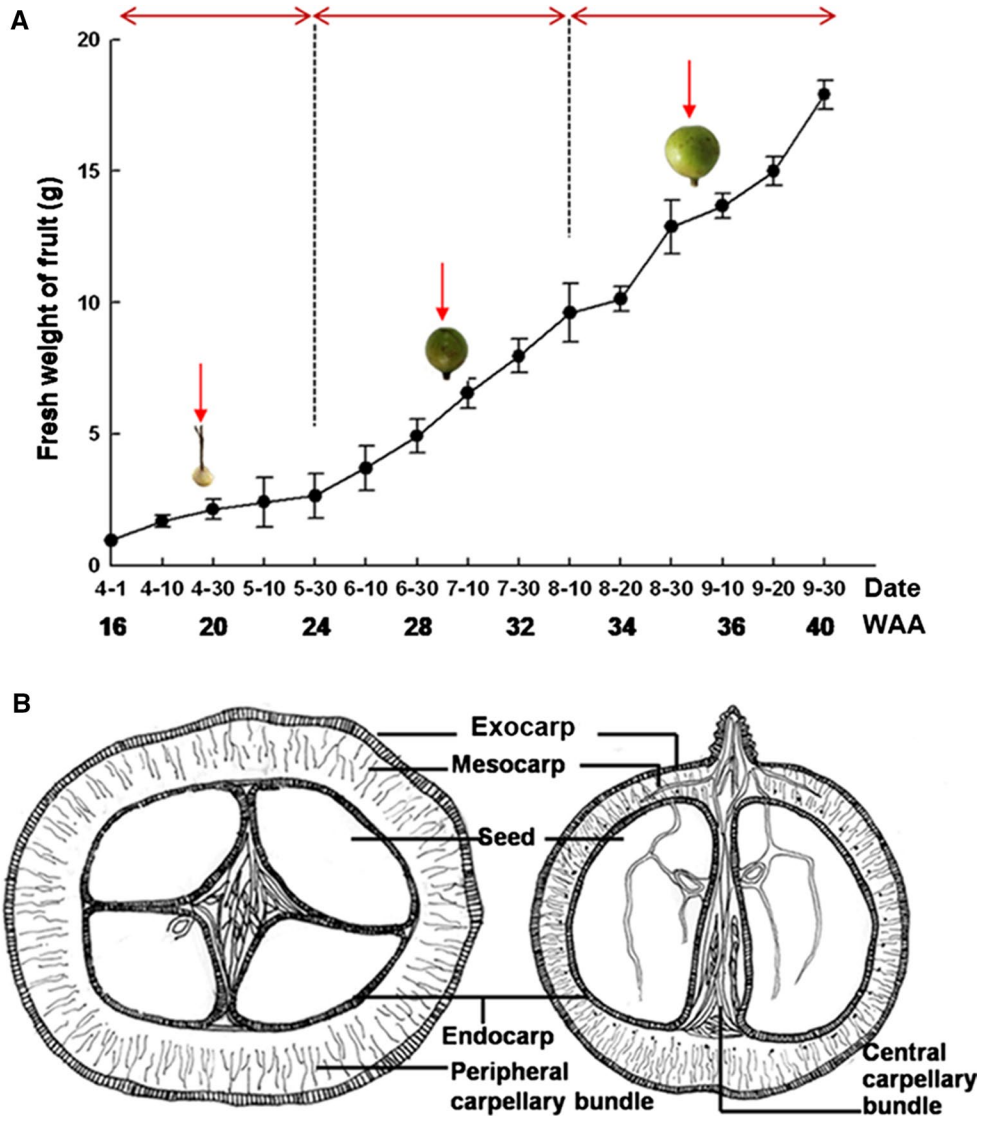

Fig. 1 Diagrammatic anatomy of *Camellia oleifera* fruit and growth curve of the variety 'xianglin 11'. **a** Developmental growth curve of 'xianglin 11'. The red arrows indicate the corresponding fruit morphology with time. **b** Transverse and longitudinal sections of fruit showed the anatomical structure of the fruit and the vascular network

phosphate buffer, the tissue cubes were post-fixed in 1% (w/v) OsO4 for 12 h at 25 °C. Subsequently, the samples were eluted with 30, 50, 70, and 95% ethanol and 100% acetone, respectively. The infiltration with Spurr into samples was carried out for 24 h at 25 °C and then polymerization for 8 h at 68 °C. Microtome (LEICAU6i) was used to prepare thick pieces (60–90 nm). The ultrathin sections were put onto the cooper grid with 100 meshes which were previously covered with 0.25% Formvar film. JEM-1010 transmission electron microscope was used for the ultrastructure observation.

Measurement of plasmodesmal frequency and density

The plasmodesmal density was measured according to (Nie et al. 2010). Continuous serial slices were prepared with microtome and the interval between serial slices is approximately 15–20 mm. For the plasmodesmal density and frequency measurement, six pieces of ultrathin section were picked randomly. Five SE–CC complexes are selected as the central field of vision. The density and frequency of plasmodesmata on the cell interfaces such as SE–CC, SE (CC)–PP, and PP–PP was statistically analyzed. The plasmodesmal density is simply counted by the number of plasmodesmata divided by specific cell–cell interface distance.

CF transport and Texas-Red Labeling

CF is a kind of fluorescent marker for phloem unloading. Carboxyfluorescein diacetate (CFDA) different from membrane-impermeable CF is non-fluorescent and membrane permeable. When CFDA is loaded into cells, it is degraded to fluorescent CF. The experiment was carried out according to Zhang et al. (2004). Briefly, the thin thread was crossed through one Eppendorf tube and the wads of cotton was put

into the tube. Then, use the needle carefully through the phloem and drop proper amount of EDTA (2.5 mmol/L) into the wound. Subsequently, 150 µL of 1 mg/mL CFDA solution was added into the tube. CF was allowed to translocate in plant for 48–72 h. The treated fruits were immediately sectioned after harvest and examined by CLSM.

To clearly mark the position of the xylem, when the CFDA-treated fruits were harvested, the pedicel was immersed into 3-kD Texas-Red dextran solution immediately and absorbed for 40 min by transpiration pull. The treated fruits were sectioned for examination under CLSM. Occasionally, to promote the absorption process and overcome the high resistance of xylem in pedicel, the fruits treated with CFDA were sliced first, and then immersed in 3-kD Texas-Red dextran solution. When examined, the part that was not immersed in the solution was cut into slices for observation.

The phloem or xylem of treated fruits was cut into transverse or longitudinal sections by hand-sliced method and the slices were immediately immersed into 80% (v/v) glycerol for CLSM observation.

Microscopy observation

CF transport was observed with a Leica SP8 confocal laser-scanning microscope with excitation of 488 nm. For those fruits, in which Texas-Red dextran and CF were simultaneously introduced, the sections were imaged first under blue (488 nm) light for CF and then under green excitation (568 nm) light for Texas-Red dextran.

Extraction and analysis of enzyme

The enzyme extraction and activity assays of SAI and CWI were essentially conducted according to (Pan et al. 2005) with modification. Briefly, 1.00 g of fruit pulp was added into mortar together with 10 mL 50 mmol/L Hepes–NaOH buffer (pH 7.5), 2.5 mmol/L DTT, 10 mmol/L ascorbic acid, 10 mmol/L $MgCl_2$, 1 mmol/L EDTA, 5% (w/v) polyvinylpolypyrrolidone (PVPP), and ground into a slurry. The filtrate obtained by filtering the slurry with cheesecloth was centrifuged for 20 min at 12,000×*g*. The upper liquid was collected for assays of SAI and the residue was rinsed repeatedly with the above Hepes buffer without PVPP until there is no protein detected in the filtrate. Subsequently, the residue was gently shaked in extraction buffer supplemented with 500 mmol/L NaCl for 24 h and centrifuged, the supernatant fluid was collected for enzyme assays of CWI. Acid invertase activity was assayed as the following steps: add 1 mL reactive liquid (100 mmol/L sodium acetate buffer at pH 4.8, 100 mmol/L Suc, 5 mmol/L $MgCl_2$, 1 mmol/L EDTA) into 0.1 mL enzyme extracting solution, incubate at 35 °C for half an hour and then boil for 5 min to stop the reaction.

Determination of soluble sugar content

Briefly, 50 g fruit powders were transferred to 4 mL 80% ethanol and mixed. Then, the mixture was boiled twice for 30 min each. The supernatant was transferred to a volumetric flask after a high-speed centrifugal at 3000×*g* for 20 min. 1.5 mL DNS reagent was mixed with 2 mL extraction and boiled for 5 min in water. Then, the volume was diluted to 25 mL with distilled water. The optical density (OD) value was determined at 540 nm and the soluble sugar content was analyzed based on the standard curve of samples. HPLC was adopted for sucrose, fructose, and glucose detection. The parameters were as follows: an Agilent Technologies 1200 Series, chemical workstation version B.02.01-SR2; 6.5 × 300 mm Sugar–PakTM1 column (Waters); a refractive index detector temperature of 70 °C; ultrapure water as mobile phase, at a flow rate of 0.4 mL/min^{-1}; a column temperature of 80 °C; 20 µl. D-(+)Glc, Suc, and D-(–) Fru (Sigma-Aldrich) were injected as the standard samples. The experiments were repeated biologically three times.

Crude fat determination

The seed oil was extracted by Soxhlet extraction (Chen et al. 2006). The filter papers used in the experiment were first put into oven (105 ± 2 °C) and dried for 2 h. The dried filter paper was then weighed and marked as (*A*) after cool down to room temperature. 1 g of seed powder was loaded into the weighed filter paper and put into oven (105 ± 2 °C) and dried for 3 h. Then, the dried filter paper with seed powder was cooled down to room temperature and marked as (*B*). The powder was enclosed into extraction barrel and distilled with diethyl ether at 60 °C until petroleum ether color clarification. The sample was then taken out and make sure diethylether fully to volatilize. After dried in oven for another 2 h, the sample was weighed and marked as (*C*). The oil content was finally calculated according to the formula: oil content in dried seed (%) = $(B - C)/(B - A) \times 100$ and crude fat content = oil content × 100.

Results

The ultrastructure observation of sieve element–companion cell complex and its adjacent cells in *C. oleifera*

Camellia oleifera fruit is anatomically composed of seed and pericarp. Pericarp which is made of epicarp, mesocarp, and endocarp originates from the differentiation and development of the ovary wall. Therefore, the photoassimilate for pericarp development is fed through peripheral carpellary bundles located in the mesocarp and the central carpellary

bundles spreading all over seed coat for seed development (Fig. 1).

Ultrathin sections of vascular tissue were observed by TEM to explore the density of plasmodesmata between SE–CC complex and its adjacent parenchyma cells at fruit different phases. The results showed that plasmodesmata were almost observed between the SE–CC cells and its surrounding cells at the early and late developmental phases, whereas scarcely observed at the middle phase (Fig. 2 and Table 1). Nevertheless, between phloem parenchyma and flesh parenchyma cells, many plasmodesmata were noticed either at the early stage or middle and late stages, suggesting the extensive apoplasmic pathway in post-phloem transport.

Table 1 Plasmodesmal densities between different types of cell in phloem of peripheral carpellary bundles of *Camellia oleifera* fruit

Stage	Early	Middle	Late
SE–CC	0.74 ± 0.03b	0.67 ± 0.06b	0.53 ± 0.06b
SE–PP	0.95 ± 0.10b	0.12 ± 0.04d	0.83 ± 0.06a
CC–PP	0.73 ± 0.06b	0.36 ± 0.06c	0.81 ± 0.05a
PP–FP	1.59 ± 0.08a	1.75 ± 0.03a	0.88 ± 0.11a

The unit of PDD represents the number of plasmodesmata μm^{-1}. Data are mean ± SE ($n = 10$). Different letters suggest significant difference according to Duncan test $\alpha = 0.05$

SE sieve element, *PP* phloem parenchyma cell, *CC* companion cell, *FP* flesh parenchyma cell

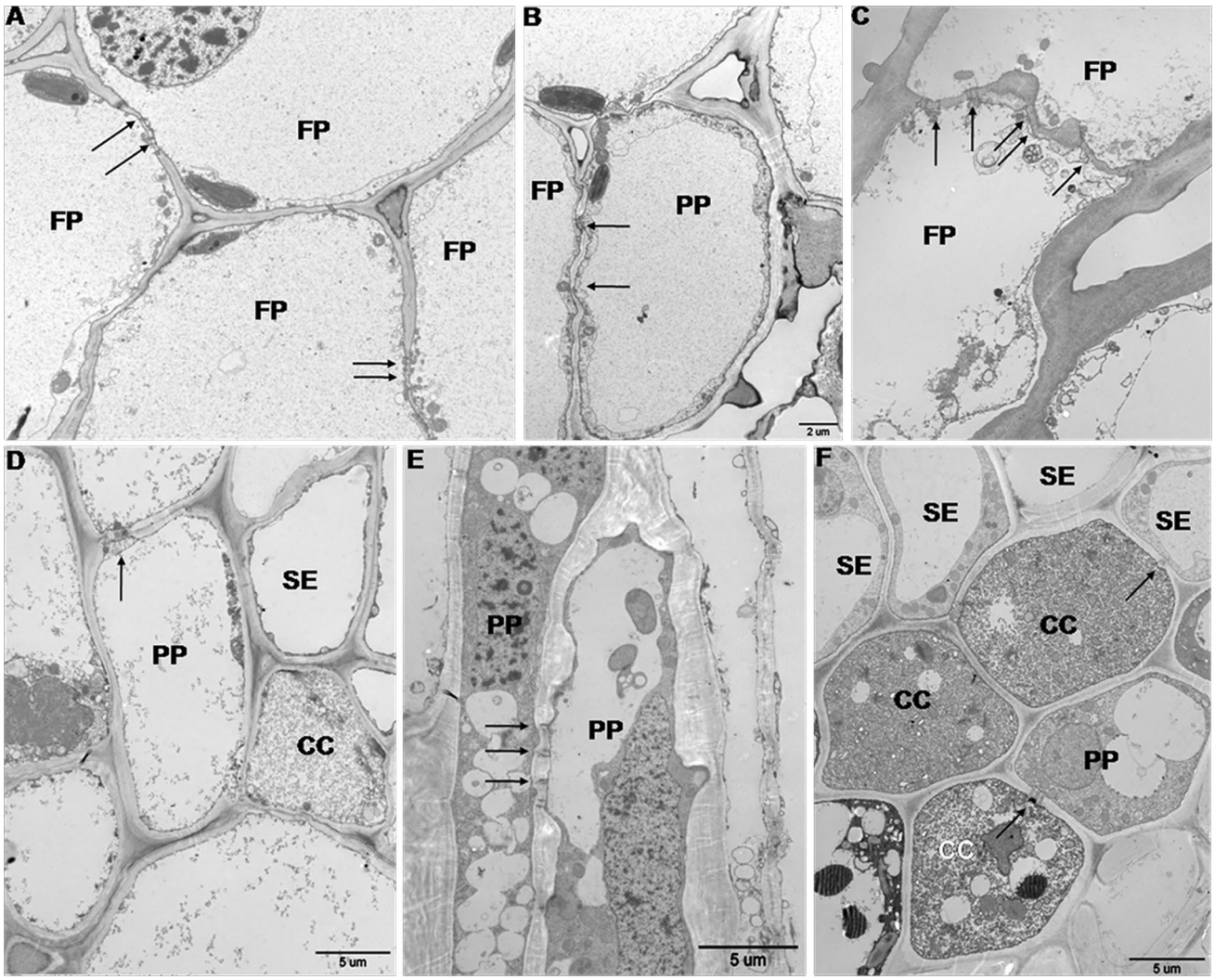

Fig. 2 Structure of phloem cells in *Camellia oleifera* fruit. **a**–**c**, and **e** Transverse or longitudinal section of phloem at different fruit development period (**a** and **b** were the early period, **c** was middle and **e** was late period). The arrows indicate the plasmodesmata between flesh cells or phloem cells. **d** Transverse section for SE–CC complex and phloem at middle stage. The arrow indicates plasmodesmata between PPs. **f** showed the branch plasmodesmata in the interface of SE–CC or CC–PP. *CC* companion cell, *SE* sieve element, *PP* phloem parenchyma cell, *FP* flesh parenchyma cell; Bars in (**a** and **c**) are the same as in (**d**)

CF transport and observation during fruit development

The distribution and unloading pattern in flesh tissue and vascular bundles are shown in Fig. 3. The fluorescent images of CF transport in fleshy pericarp showed that CF diffuses apparently out from the phloem strands, and is widely distributed in parenchyma cells around the phloem at early and late phases of fruit development. However, the fluorescent in major or minor bundles was detected only in the phloem strands at middle stage. We noticed that the first transition of phloem-unloading pathway in fleshy pericarp occurred approximately on 23rd of May (23 WAA); afterwards, the amount of CF unloading decreased, suggesting that the phloem-unloading pathway transformed from symplastic to apoplastic; the second transition of phloem unloading occurred on the 23rd of August (34 WAA); from then, the amount of CF unloading increased and suggest the transition from apoplastic to symplastic pathways (Fig. 4). In addition, the central carpellary bundles were sampled and observed for CF distribution in vascular bundles. In the seed, before endocarp hardening, whether in the longitudinal or transverse section of vascular bundle, CF was clearly spread from the phloem strands into its adjacent tissues, suggesting that the seed growth is feed by maternal tissues via symplasmic transport (supplemental Fig. 1).

To distinctly differentiate phloem from xylem and ensure CFDA transport only within phloem zone, Texas Red as a xylem vessel tracer was introduced into fruit to follow the CFDA introduction. As shown in Fig. 5, the Texas-Red

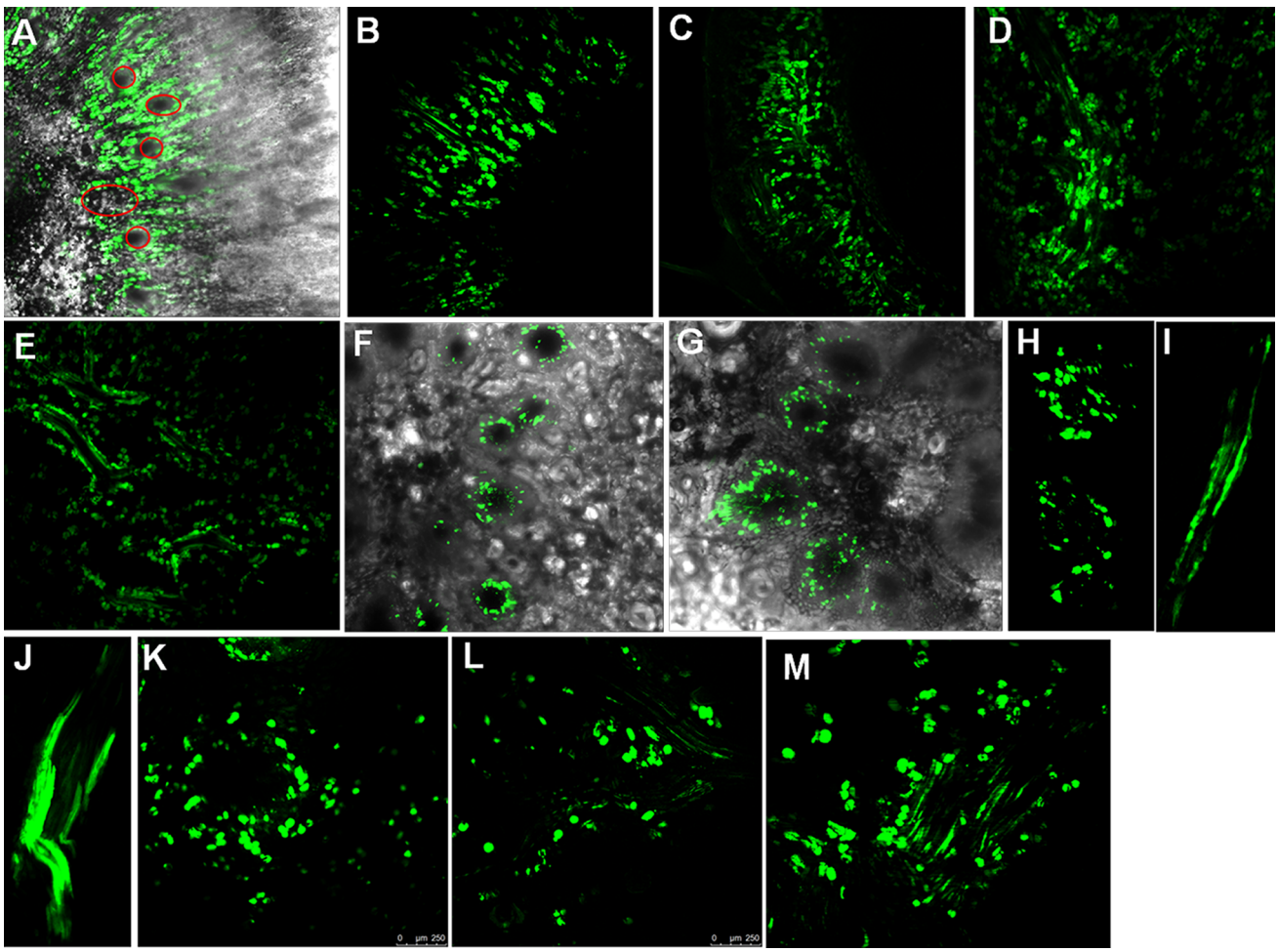

Fig. 3 CLSM observation of CF transport in phloem during *Camellia oleifera* fruit development. **a**–**e** fruits collected at early stage. **a** Transverse section adjacent to the bottom of the fruit at early stage. **a** is the overlay image of fluorescent and bright-field image. Red circle indicates the zone of vascular bundles. **b** Transverse section of whole fruit. **c** Longitudinal section of whole fruit. **d**, **e** Longitudinal section of major vascular bundle (**d**) and branched minor vascular bundle (**e**). **f**–**j** Fruits sampled at middle stage. **f**–**h** Transverse section of fleshy fruits. **i**, **j** Longitudinal section of minor and major vascular bundle, respectively. **k**–**m** Fruits sampled at late phase. **k** Transverse slice of the fleshy tissue. **l**, **m** Longitudinal section of branched minor and major vascular bundle, respectively. Bars in (*K*) = 250 μm. The bars in other images are the same to that in (K)

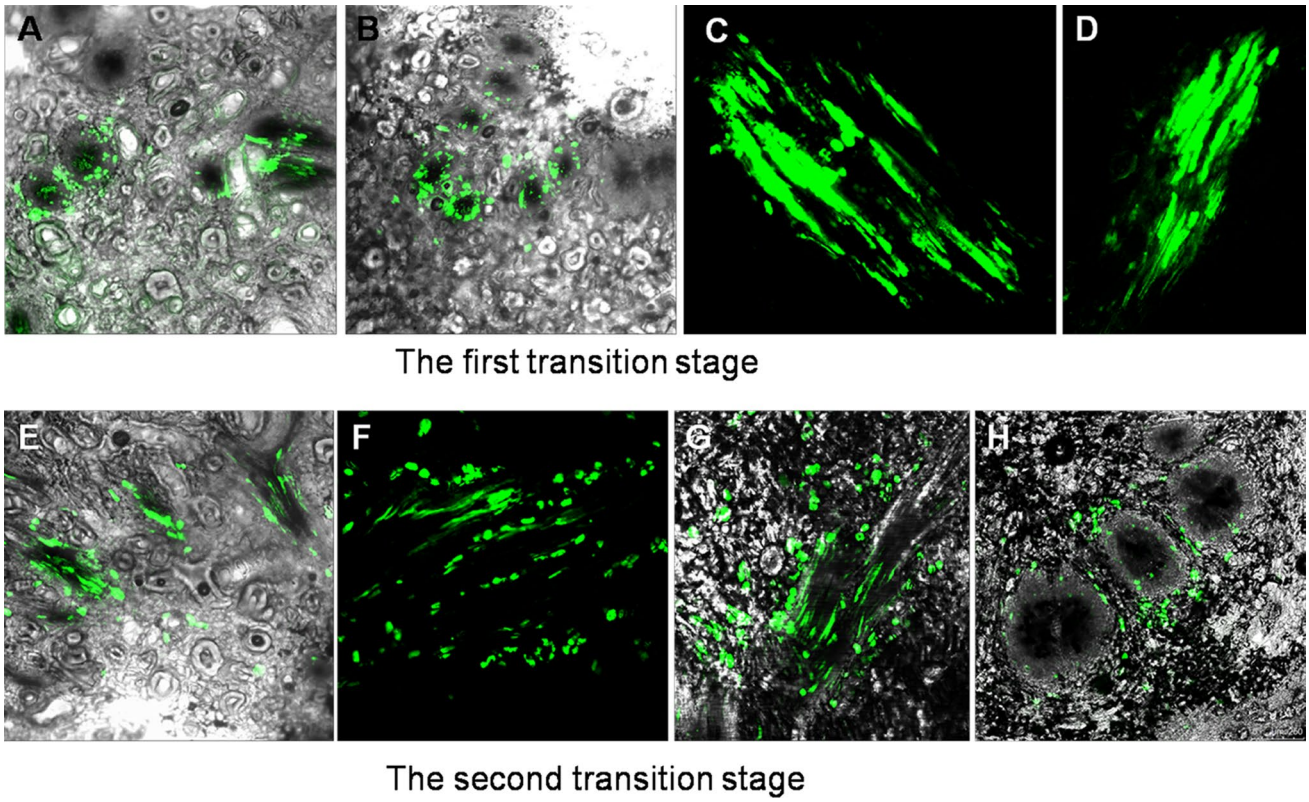

Fig. 4 Transition phloem transport pathway in the process of fruit development. **a**–**d** First transition stage. The fruits sampled on May 20th, showing that CF unloading quantity declined. **a**, **b** Transverse cut. **c**, **d** Longitudinal section. **e**–**h** Second transition stage. The fruits sampled on August 23rd, showing that CF began to exit from vascular bundle section. **e**–**g** Longitudinal section. **h** Transverse section

fluorescence (red) and CF fluorescence (green) were detected in only xylem zone and phloem zone, respectively, suggesting that the results of this study are reliable

The activity assays of acid invertase and neutral invertase during fruit development

The enzyme activities of acid invertase and neutral invertase were measured at different fruit stages (Fig. 6c). The cell wall invertase showed a higher enzymatic activity than soluble acid invertase at the early fruit developmental stage and reached the highest level of 24 mg g^{-1} h^{-1} at 25 WAA and then sharply decreased until another high level at late stage. The enzymatic activity of soluble acid invertase exceeds that of cell wall invertase and showed the highest level at late stage. It is obvious that the enzymatic activity of the two kinds of acid invertase varied in a reverse pattern, whereas the activity of neutral invertase showed little change during the whole fruit development.

The analysis of oil accumulation and content of soluble sugar

Camellia oleifera fruit undergoes three major developmental stages: early developmental stage, fast growing stage, and oil accumulation and fruit full-blown stage. To explore the possible relationship between oil accumulation and soluble sugar, the content of both was determined. As shown in Fig. 6, the content of soluble sugar greatly increased at the early stage, peaked at 26 WAA, and then dropped significantly. In contrast, the oil content increased significantly since August 29 (~ 35 WAF). Oil rapid accumulation began September 6th (~ 36 WAF) and continued to rise until harvest. With the oil accumulation, the content of soluble sugar declined sharply. Furthermore, we analyzed the correlation of soluble sugar content with oil accumulation in mesocarp and seeds. We found that the lipid accumulation with content of soluble sugar was significantly negatively correlated at $P < 0.05$ level. However, SAI, CAI, or NI showed a significant

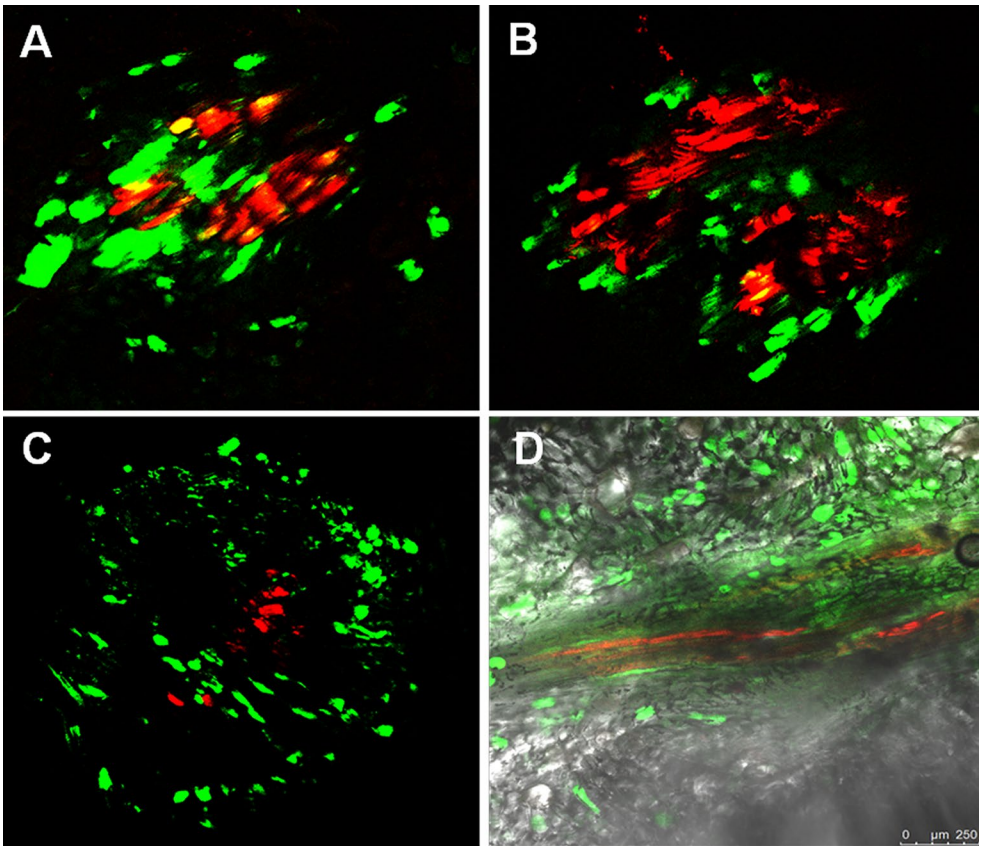

Fig. 5 CLSM imaging of CF and Texas-Red dextran. CF and Texas-Red dextran were introduced into phloem and xylem of fruit, respectively, according to the "Materials and methods". CF was trapped in the phloem of major bundle in fruit adjacent to the pedicle (**a**, **b**). **c**, **d** Transverse (**c**) and longitudinal (**d**) section of minor bundle. **a**, **b**, and **d** are from the fruits during the middle developmental stage; **d** is from the fruit at the late stage. The red strands and areas indicate the xylem zone. Bars in (*D*) = 250 μm. The bars in (**a**, **b**, **c**) are the same to that in (**d**)

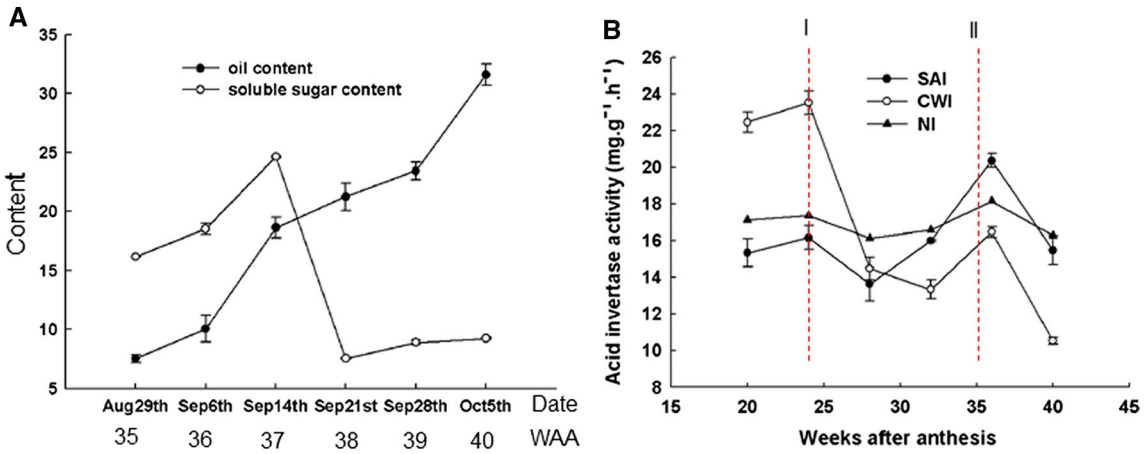

Fig. 6 Changes of soluble sugar and oil content and acid invertase activity during fruit development. **a** Oil content in seed and sugar content in fleshy mesocarp at oil accumulation stage. The unit of oil content is % and the unit of soluble sugar content is mg g^{-1} fresh weight. **b** Change of invertase activity. The red line represents the first and second transitions, respectively

Table 2 Correlation analysis of oil content and soluble sugar content and invertase

Index	Soluble sugar content	SAI	CWI	NI
Oil content	− 0.774*	0.893**	0.809**	0. 856**

SPASS 20.0 software was used for correlation analysis

Pearson correlation coefficient method was used for the correlation analysis

* indicates significance at 0. 05 level

** indicates significance at 0. 01 level

positive correlation with lipid accumulation at $P < 0.01$ level (Table 2).

Discussion

The shift of phloem-unloading pattern of sucrose in *C. oleifera* fruit

In the present study, we found that the complex of SE–CC is interconnected to the surrounding cells by plasmodesmata during early or late developmental phases of fruit, which provides a symplasmic transport channels (Fig. 2, Table 1). However, the absence of plasmodesmata at the middle stage in *C. oleifera* fruit showed the symplasmic isolation between the complex of SE–CC and parenchyma cells. Real-time imaging of CF transport in phloem zone further confirmed the symplasmic continuum through plasmodesmata during early and late stages (Fig. 3). These results suggested that sucrose was transported via symplast system in the early and late phases, whereas apoplast system in middle stage during *C. oleifera* fruit development. The same results were observed for both the variety 'xianglin 11' and 'xianglin 78' (data not shown), further demonstrating that physiological changes has an effect on the phloem-unloading pathways which were complicated during fruit development. However, the routes of phloem unloading did not differ among different varieties for the same species.

Acid invertase (EC 3.2.1.26) exists in two forms, including soluble form and insoluble form. Soluble acid invertase is found in vacuole regulating the accumulation of sugar in the fruit and the use of sucrose in the vacuole. However, insoluble acid invertase is attached to the cell wall (Quick and Schaffer 1996). Here, we found that the two forms of acid invertase had a great discrepancy at the early and late phases and slight difference at the middle stage of fruit development, whereas neutral invertase changed a little. Interestingly, cell wall invertase activity reached the highest at the onset of middle stage of fruit development, supporting the apoplastic unloading pathway. The acid invertase exists in cell wall, providing a potential mechanism for sucrose degraded and transported from phloem to the apoplast. It is reported that acid invertases participate in the decomposition of sucrose and promote the unloading of the source during the apoplasmic unloading of phloem. (Patrick 1997). In jujube fruit, cell wall invertase existed mainly in the complex SE–CC and the parenchyma cells and showed substantial increase during fruit development (Nie et al. 2010). Here, we also found the high activity of soluble acid invertase and neutral invertase at the late period of fruit development, which probably led to the maintenance of turgor in the vacuole and sugar accumulations to facilitate fruit maturation and oil accumulation.

The unloading mechanism of fast-developing terminal sink

In tomato, sucrose was transported via symplast system at the early period, but apoplasmic route at the late fruit development phase (Patrick and Offler 1996; Ruan and Patrick 1995). In grape berry, the phloem-unloading pathway changed from symplasmic to apoplasmic at earlier stages of ripening (Zhang et al. 2006). In *Ziziphus jujuba*, the transition in sym- and apoplasmic pathways were also observed throughout fruit development (Nie et al. 2010). Here, we observed symplasmic unloading pattern at the early and late periods and apoplasmic unloading pattern at middle period during *C. oleifera* fruit development. These results suggest the universality of the transition of phloem-unloading route in fruit sinks, implying the complexity of photoassimilate transport and unloading mechanism in fruit sink compared to vegetative sink tissues. There is no doubt that the decrease in plasmodesmata number and density is the major reason for the decline of symplasmic unloading capacity in *C. oleifera* fruit. Compared to other species such as apple, which has more plasmodesmata between different cell types (Zhang et al. 2004), *C. oleifera* fruit has a low level of plasmodesmata number and density either at the interface of SE–CC or SE/CC with PP even at early and late developmental phases of fruit when symplasmic transport is predominant. Interestingly, we once observed golden particles representing hexose transporter in plasmodesmata zone on the interface of SE–CC complexes in apple fruit via immunogold electron microscopy (data not published). Recently, Milne et al. found that SbSUT1 and SbSUT5 were immune localized to sieve element in elongating internodes and storage parenchyma cells (Milne et al. 2017). It is likely that sugar transporters function, on one hand, in sucrose retrieval into sieve element to keep a high turgor which contributed to the forming of bulk flow and drive symplasmic unloading; on the other hand, the symplasmic unloading predominates jointly by sugar transporters making up for the deficiency of plasmodesmata transport ability in fast-developing terminal sinks.

The increase of CWI expression and activity from the onset of ripening to the late stage further proved an apoplasmic pattern after the onset of ripening of grape (Hayes et al. 2007; Zhang et al. 2006). However, in *C. oleifera* fruit, the first and second transitions of phloem-unloading route occurred during 23 WAA and 34 WAA, respectively, when is approximately the onset and end of the middle developmental stage. The activity of CWI reached the highest at the first transition (from sym- to apoplastic) and then declined and afterwards reached another high level at the second transition (Fig. 6), suggesting the role of CWI the transition of phloem-unloading route. Indeed, high activity of invertase is not only related to rapid growth of tissue, the formation of sucrose content gradient, fruit development, and sugar accumulation, but also fruit set. Cell wall invertase (CWIN) LIN5 was reported to function exclusively in SEs walls and enhance its activity during ovary-to-fruit transition in tomato (Palmer et al. 2015), probably facilitating sucrose unloading and forming a glucose signal during cell division and the development of fruit set stage. These data suggest that CWI is not only involved in facilitating apoplasmic unloading, but also the transition process of phloem unloading during fruit set and development. Compared to CWI and SAI which showed a great change, NI remained relative high activity and changed little during fruit development. Nevertheless, SAI, which had a higher enzyme activities at late developmental stage, plays active role in sucrose metabolism in vacuole (Nguyen-Quoc and Foyer 2001).

The mechanism of fatty acid biosynthesis in *C. oleifera* seed

The acetyl-CoA is the basic material for fatty acid synthesis, which mainly comes from glycolysis product pyruvic acid (Salas et al. 2000). Therefore, the accumulation and metabolism of sugar provide fundamental material and precursor for fatty acid biosynthesis. In olive, the sugar accumulation occurred within 60 days after anthesis and provided material basis and precursor for oil biosynthesis (Cheng et al. 2014). The oil biosynthesis occurred at 36 WAA and a great amount of oil was synthesized especially after 37 WAA in *C. oleifera*. Meanwhile, sugar content sharply declined, suggesting the active sugar metabolism and transition between sugar and fat (Fig. 6). The correlation analysis showed that the lipid accumulation was significantly negatively correlated with content of soluble sugar $P < 0.05$ level, suggesting that the degradation of sucrose accelerates oil accumulation.The correlation analysis showed that a significant positive correlation occurred between acid invertase and neutral invertase and lipid accumulation (Table 2), suggesting that invertase plays positive roles in fatty acid biosynthesis by degrading sucrose into glucose and fructose in *C. oleifera*. Nevertheless, further work should be focused on the molecular mechanisms of sucrose transporter/hexose transporter, invertase, and fatty acid synthesis and would be of great significance in exploring the strategy plant evolved and elucidating the correlation between sucrose metabolism and oil accumulation.

Author contribution statement XW carried out the experiment and analyzed the data; HY plotted the data and edited the references; YY and HZ revised the manuscript; and LZ designed the experiment and wrote the manuscript.

Acknowledgements We thank Dr. Yongzhong Chen and Rui Wang at the Forestry Research Institute of Hunan Province in China, for their kind help in providing the testing ground and plant materials. This work was supported by a grant from National Key Project of "11th five-year plan" science and technology support plan (Grant No. 2009BADB0401.).

References

Aoki N, Scofield GN, Wang XD, Offler CE, Patrick JW, Furbank RT (2006) Pathway of sugar transport in germinating wheat seeds. Plant Physiol 141:1255–1263. https://doi.org/10.1104/pp.106.082719

Chen YZ, Xiao ZH, Peng SF, Yang XH, Li DX, Wang XN, Duan W (2006) Study of fruit growing specialties and its oil content in oil–tea camellia. For Res 19:9–14. https://doi.org/10.3321/j.issn:1001-1498.2006.01.002

Chen LQ et al (2015) A cascade of sequentially expressed sucrose transporters in the seed coat and endosperm provides nutrition for the Arabidopsis embryo. Plant Cell 27:607–619. https://doi.org/10.1105/tpc.114.134585

Chen C, Yuan YL, Zhang C, Li HX, Ma FW, Li MJ (2017) Sucrose phloem unloading follows an apoplastic pathway with high sucrose synthase in Actinidia fruit. Plant Sci 255:40–50. https://doi.org/10.1016/j.plantsci.2016.11.011

Cheng ZZ, He JS, Zhan MM et al (2014) Synthesis of olive oil during olive oevelopment and ripening. Sci Silvae Sin 50(5):123–131

Haupt S, Duncan GH, Holzberg S, Oparka KJ (2001) Evidence for symplastic phloem unloading in sink leaves of barley. Plant Physiol 125:209–218

Hayes MA, Davies C, Dry IB (2007) Isolation, functional characterization, and expression analysis of grapevine (*Vitis vinifera* L.) hexose transporters: differential roles in sink and source tissues. J Exp Bot 58:1985–1997. https://doi.org/10.1093/jxb/erm061

Imlau A, Truernit E, Sauer N (1999) Cell-to-cell and long-distance trafficking of the green fluorescent protein in the phloem and symplastic unloading of the protein into sink tissues. Plant Cell 11:309–322

Milne RJ et al (2017) Sucrose transporter localization and function in phloem unloading in developing stems. Plant Physiol 173:1330–1341. https://doi.org/10.1104/pp.16.01594

Nergiz C, Ergonul PG (2009) Organic acid content and composition of the olive fruits during ripening and its relationship with oil and sugar. Sci Hortic-Amsterdam 122:216–220. https://doi.org/10.1016/j.scienta.2009.05.011

Nguyen-Quoc B, Foyer CH (2001) A role for 'futile cycles' involving invertase and sucrose synthase in sucrose metabolism of tomato fruit. J Exp Bot 52:881–889

Nie P, Wang X, Hu L, Zhang H, Zhang J, Zhang Z, Zhang L (2010) The predominance of the apoplasmic phloem-unloading pathway is interrupted by a symplasmic pathway during Chinese jujube fruit development. Plant Cell Physiol 51:1007–1018. https://doi.org/10.1093/pcp/pcq054

Oparka KJ (1990) What is phloem unloading? Plant Physiol 94:393–396

Oparka KJ, Cruz SS (2000) The great escape: phloem transport and unloading of macromolecules. Annu Rev Plant Physiol Plant Mol Biol 51:323–347

Palmer WM, Ru L, Jin Y, Patrick JW, Ruan YL (2015) Tomato ovary-to-fruit transition is characterized by a spatial shift of mRNAs for cell wall invertase and its inhibitor with the encoded proteins localized to sieve elements. Mol Plant 8:315–328. https://doi.org/10.1016/j.molp.2014.12.019

Pan QHZK, Peng CC, Wang XL, Zhang DP (2005) Purification, biochemical and immunological characterization of acid invertases from apple fruit. J Integr Plant Biol 47:50–59

Patrick JW (1997) Phloem unloading: sieve element unloading and post-sieve element transport. Ann Rev Plant Physiol Plant Mol Biol 48:191–222. https://doi.org/10.1146/annurev.arplant.48.1.191

Patrick JW, Offler CE (1996) Post-sieve element transport of photoassimilates in sink regions. J Exper Bot. https://doi.org/10.1093/jxb/47.special_issue.1165

Quick W, Schaffer A (1996) Sucrose metabolism in sources and sinks. In: Zamski E, Schaffer AA (eds) Photoassimilate distribution in plants and crops: source–sink relationships. Marcel DekkerInc, New York, pp 115–156

Ruan YL, Patrick JW (1995) The cellular pathway of post-phloem sugar transport in developing tomato fruit. Planta 196:434–444

Salas JJ, Sanchez J, Ramli US, Manaf AM, Williams M, Harwood JL (2000) Biochemistry of lipid metabolism in olive and other oil fruits. Prog Lipid Res 39:151–180

Turgeon R, Wolf S (2009) Phloem transport: cellular pathways and molecular trafficking. Annu Rev Plant Biol 60:207–221. https://doi.org/10.1146/annurev.arplant.043008.092045

Viola R et al (2001) Tuberization in potato involves a switch from apoplastic to symplastic phloem unloading. Plant Cell 13:385–398

Wang XY, Cao YB, Zhang LY, Chen YZ (2012) Analysis of the fatty acids compositions of Camellia in different growth stages. Chin Agric Sci Bull 28:76–80

Wang TD, Zhang HF, Wu ZC, Li JG, Huang XM, Wang HC (2015) Sugar uptake in the Aril of litchi fruit depends on the apoplasmic post-phloem transport and the activity of proton pumps and the putative transporter LcSUT4. Plant Cell Physiol 56:377–387. https://doi.org/10.1093/pcp/pcu173

Zanon L, Falchi R, Santi S, Vizzotto G (2015) Sucrose transport and phloem unloading in peach fruit: potential role of two transporters localized in different cell types. Physiol Plant 154:179–193. https://doi.org/10.1111/ppl.12304

Zeng QL, Chen RF, Zhao XQ, Shen RF, Noguchi A, Shinmachi F, Hasegawa I (2013) Aluminum could be transported via phloem in *Camellia oleifera* Abel. Tree Physiol 33:96–105. https://doi.org/10.1093/treephys/tps117

Zhang LY et al (2004) Evidence for apoplasmic phloem unloading in developing apple fruit. Plant Physiol 135:574–586. https://doi.org/10.1104/pp.103.036632

Zhang XY et al (2006) A shift of phloem unloading from symplasmic to apoplasmic pathway is involved in developmental onset of ripening in grape berry. Plant Physiol 142:220–232. https://doi.org/10.1104/pp.106.081430

Zhang HH, Li YF, Nie PX, Wang HY, Zhang LY (2016) Phloem unloading pathway of photosynthates and sucrose-metabolizing enzymes activities in vaccinium corymbosum Fruit. SCIENTIA SILVAE SINICAE 53:40–48